

V.V. SAGUN,<sup>1</sup> D.R. OLIINYCHENKO,<sup>1,2</sup> K.A. BUGAEV,<sup>1</sup> J. CLEYMANS,<sup>3</sup>  
 A.I. IVANYTSKYI,<sup>1</sup> I.N. MISHUSTIN,<sup>2,4</sup> E.G. NIKONOV<sup>5</sup>

<sup>1</sup> Bogolyubov Institute for Theoretical Physics, Nat. Acad. of Sci. of Ukraine  
 (14b, Metrolohichna Str., Kyiv 03680, Ukraine; e-mail: v\_sagun@ukr.net,  
 bugaev@th.physik.uni-frankfurt.de, a\_iv\_@ukr.net )

<sup>2</sup> FIAS, Goethe-University  
 (1, Ruth-Moufang Str., Frankfurt am Main 60438, Germany; e-mail: dimafopf@gmail.com,  
 mishustin@fias.uni-frankfurt.de)

<sup>3</sup> Department of Physics, University of Cape Town  
 (Rondebosch 7701, South Africa; e-mail: jean.cleymans@uct.ac.za)

<sup>4</sup> Kurchatov Institute, Russian Research Center  
 (Kurchatov Sqr., Moscow 123182, Russia)

<sup>5</sup> Laboratory for Information Technologies, JINR  
 (Dubna 141980, Russia; e-mail: e.nikonov@jinr.ru)

## STRANGENESS ENHANCEMENT AT THE HADRONIC CHEMICAL FREEZE-OUT

PACS 25.75.-q, 25.75.Nq

---

*The chemical freeze-out of hadrons created in the high energy nuclear collisions is studied within a realistic version of the hadron resonance gas model. The chemical non-equilibrium of strange particles is accounted via the usual  $\gamma_s$  factor, which gives us an opportunity to perform a high quality fit with  $\chi^2/\text{dof} \simeq 63.5/55 \simeq 1.15$  of the hadronic multiplicity ratios measured from the low AGS to the highest RHIC energies. In contrast to the previous findings, we observe the strangeness enhancement at low energies instead of a suppression. In addition, the performed  $\gamma_s$  fit allows us to achieve the highest quality of the Strangeness Horn description with  $\chi^2/\text{dof} = 3.3/14$ . For the first time, the top point of the Strangeness Horn is perfectly reproduced, which makes our theoretical horn as sharp as an experimental one. However, the  $\gamma_s$  fit approach does not sizably improve the description of the multistrange baryons and antibaryons. Therefore, an apparent deviation of the multistrange baryons and antibaryons from the chemical equilibrium requires a further explanation.*

*Keywords:* chemical freeze-out,  $\gamma_s$  factor, Strangeness Horn, hadron multiplicities.

### 1. Introduction

The hadron yields measured in heavy ion collisions are traditionally analyzed within the Hadron Resonance Gas Model (HRGM) [1–4]. Its main assumption is the existence of a thermal equilibrium in the system under consideration, which is strongly supported by the excellent coincidence of experimental

and theoretical yields of the hadrons built up from  $u$  and  $d$  quarks. Using the temperature  $T$ , baryonic chemical potential  $\mu_B$ , and chemical potential of the isospin third component  $\mu_{I3}$ , the HRGM allows one to describe the hadronic multiplicities at the moment of chemical freeze-out (FO), the moment at which all inelastic reactions cease to exist. However, the HRGM has some traditional problems in the description of the strange hadrons. Thus, within the standard HRGM formulation with a single hard-core repulsion radius for all particles, the energy dependences

© V.V. SAGUN, D.R. OLIINYCHENKO, K.A. BUGAEV,  
 J. CLEYMANS, A.I. IVANYTSKYI, I.N. MISHUSTIN,  
 E.G. NIKONOV, 2014

of  $K^+/\pi^+$  and  $\Lambda/\pi^-$  ratios were never satisfactorily reproduced [1–3]. However, the non-monotonic energy dependence of the  $K^+/\pi^+$  ratio known as the Strangeness Horn is of special interest, because it may serve as a signal of the onset of the deconfinement. In order to account for a deviation from the chemical equilibrium of strange hadrons, the factor  $\gamma_s$  was introduced [5]. It is used to describe the undersaturated (oversaturated) densities  $\gamma_s < 1$  ( $\gamma_s > 1$ ) of each strange charge. Formally, the strange fugacity associated with each (anti)strange charge is simply multiplied by the  $\gamma_s$  factor. Although the  $\gamma_s$  factor plays an important role in the analysis of the data measured in the collisions of elementary particles [3] and in the nucleus-nucleus collisions [3, 6], the problem of its justification remains unsolved. Moreover, the results on the  $\gamma_s$  values obtained within different thermal models are controversial. For instance, a strong suppression of the strange charge in nucleus-nucleus collisions was reported in Ref. [3], while the results of Ref. [6] are consistent with  $\gamma_s = 1$ . In order to resolve the latter problem, we apply the most successful version of the HRGM with multicomponent hard-core repulsion [4, 7–10] to describe 111 independent hadron yield ratios measured at 14 values of the center of mass collision energy  $\sqrt{s_{NN}}$  in the interval from 2.7 GeV to 200 GeV.

The work is organized as follows. In the next section, we give the theoretical basis of the present model. In Section 3, we present the data descriptions and discuss them. Section 4 is devoted to our conclusions.

## 2. Hadron Resonance Gas Model

We employ a multicomponent HRGM, which currently provides the best description of the observed hadronic multiplicities. It is the model developed in [4, 7–10]. The hadron interaction is taken into account via the hard-core repulsion, whose radii have different values for pions  $R_\pi$ , kaons  $R_K$ , other mesons  $R_m$ , and baryons  $R_b$ . The best global fit of all hadronic multiplicities was found for  $R_b = 0.2$  fm,  $R_m = 0.4$  fm,  $R_\pi = 0.1$  fm,  $R_K = 0.38$  fm [4]. The main equations of this HRGM are listed below, but more details can be found in [4, 7–10].

Let us consider the Boltzmann gas of  $N$  hadron species in a volume  $V$  that has the temperature  $T$ , baryonic chemical potential  $\mu_B$ , strange chemical po-

tential  $\mu_S$ , and chemical potential of the isospin third component  $\mu_{I3}$ . The pressure  $p$  and the  $K$ -th charge density  $n_i^K$  ( $K \in \{B, S, I3\}$ ) of the  $i$ -th hadron sort are given by the expressions

$$\frac{p}{T} = \sum_{i=1}^N \xi_i, \quad n_i^K = \frac{Q_i^K \xi_i}{1 + \frac{\xi^T \mathcal{B} \xi}{\sum_{j=1}^N \xi_j}}, \quad \xi = \begin{pmatrix} \xi_1 \\ \xi_2 \\ \dots \\ \xi_N \end{pmatrix}, \quad (1)$$

where  $\mathcal{B}$  denotes a symmetric matrix of the second virial coefficients with the elements  $b_{ij} = \frac{2\pi}{3}(R_i + R_j)^3$ , and the variables  $\xi_i$  are the solutions of the system

$$\xi_i = \phi_i(T) \exp \left[ \frac{\mu_i}{T} - \sum_{j=1}^N 2\xi_j b_{ij} + \xi^T \mathcal{B} \xi \left[ \sum_{j=1}^N \xi_j \right]^{-1} \right], \quad (2)$$

$$\phi_i(T) = \frac{g_i}{(2\pi)^3} \int \exp \left( -\frac{\sqrt{k^2 + m_i^2}}{T} \right) d^3k. \quad (3)$$

Here, the full chemical potential of the  $i$ -th hadron sort  $\mu_i \equiv Q_i^B \mu_B + Q_i^S \mu_S + Q_i^{I3} \mu_{I3}$  is expressed in terms of the corresponding charges  $Q_i^K$  and their chemical potentials,  $\phi_i(T)$  denotes the thermal particle density of the  $i$ -th hadron sort of mass  $m_i$  and degeneracy  $g_i$ , and  $\xi^T$  denotes the row of variables  $\xi_i$ . For each collision energy, the fitting parameters are the temperature  $T$ , baryonic chemical potential  $\mu_B$ , and chemical potential of the third projection of isospin  $\mu_{I3}$ , whereas the strange chemical potential  $\mu_S$  is found from the condition of vanishing strangeness.

In order to account for the possible strangeness non-equilibration, we introduce the  $\gamma_s$  factor in a conventional way [5] by replacing  $\phi_i$  in Eqs. (2) and (3) as

$$\phi_i(T) \rightarrow \phi_i(T) \gamma_s^{s_i}, \quad (4)$$

where  $s_i$  is the number of strange valence quarks plus the number of strange valence anti-quarks.

The width correction is taken into account by averaging all expressions containing the mass with the Breit–Wigner distribution having a threshold. As a result, the modified thermal particle density of the  $i$ -th hadron sort acquires the form

$$\int \exp \left( -\frac{\sqrt{k^2 + m_i^2}}{T} \right) d^3k \rightarrow$$

$$\rightarrow \frac{\int_{M_0}^{\infty} \frac{dx}{(x-m_i)^2 + \Gamma_i^2/4} \int \exp\left(-\frac{\sqrt{k^2+x^2}}{T}\right) d^3k}{\int_{M_0}^{\infty} \frac{dx}{(x-m_i)^2 + \Gamma_i^2/4}}. \quad (5)$$

Here,  $m_i$  denotes the mean mass of hadrons, and  $M_0$  stands for the threshold in the dominant decay channel. The main advantages of this approximation are a simplicity of its realization and a clear way to account for the finite width of hadrons. The effect of the vanishing width of resonances or the Gaussian resonance width parametrization on the chemical FO parameters is discussed in [11].

The effect of the resonance decay  $Y \rightarrow X$  on the final hadronic multiplicity is taken into account as  $n^{\text{fin}}(X) = \sum_Y BR(Y \rightarrow X)n^{\text{th}}(Y)$ , where  $BR(X \rightarrow X) = 1$  for the sake of convenience. The masses, widths, and strong decay branchings of all experimentally known hadrons were taken from the particle tables used by the thermodynamic code THERMUS [12].

### 3. Results

#### 3.1. Data sets and fit procedure

In this work, we use the data set which is identical to that in Ref. [10]. At the AGS energies ( $\sqrt{s_{NN}} = 2.7$ –4.9 GeV or  $E_{\text{lab}} = 2$ –10.7 GeV per nucleon), the data are available with a good energy resolution above 2 GeV per nucleon. However, for the beam energies 2, 4, 6, and 8 GeV per nucleon only a few data points are available. They correspond to the yields for pions [13, 14], protons [15, 16], and kaons [14] (except for 2 GeV per nucleon). The data integrated over  $4\pi$  are also available for  $\Lambda$  hyperons [17] and for  $\Xi^-$  hyperons (for 6 GeV per nucleon only) [18]. However, as it was argued in Ref. [2], the data for  $\Lambda$  and  $\Xi^-$  should be recalculated for the mid-rapidity. Therefore, instead of raw experimental data, we used the corrected values from [2]. Further, we analyzed the data set at the highest AGS energy ( $\sqrt{s_{NN}} = 4.9$  GeV or  $E_{\text{lab}} = 10.7$  GeV per nucleon). Similarly to [4], we analyze here only the NA49 mid-rapidity data [19–24] as the most difficult ones to be reproduced. Since the RHIC high energy data of different collaborations agree well with each other, we analyze the STAR results for  $\sqrt{s_{NN}} = 9.2$  GeV [25],  $\sqrt{s_{NN}} = 62.4$  GeV [26], and  $\sqrt{s_{NN}} = 130$  GeV [27–30] and 200 GeV [30–32].

The fit criterion is the minimization of  $\chi^2 = \sum_i \frac{(r_i^{\text{theor}} - r_i^{\text{exp}})^2}{\sigma_i^2}$ , where  $r_i^{\text{theor}}$  and  $r_i^{\text{exp}}$  are, respec-

tively, theoretical and experimental values of particle yield ratios,  $\sigma_i$  stands for the corresponding experimental error, and the summation is performed over all available experimental points.

#### 3.2. The $\gamma_s$ fit

To improve the description of the strange hadrons and to investigate the role of their chemical non-equilibrium within the multicomponent HRGM, we consider the  $\gamma_s$  factor as a fitting parameter for each value of collision energy. In our analysis, we pay a special attention to the  $K^+/\pi^+$  ratio, because it is usually considered as the most problematic one for the HRGM.

For 14 collision energies  $\sqrt{s_{NN}} = 2.7, 3.3, 3.8, 4.3, 4.9, 6.3, 7.6, 8.8, 9.2, 12, 17, 62.4, 130,$  and 200 GeV, the resulting fit quality  $\chi^2/\text{dof} = 63.4/55 = 1.15$  became slightly better compared to the result  $\chi^2/\text{dof} = 80.5/69 = 1.16$  found for the chemical FO model with  $\gamma_s = 1$ , although the value of  $\chi^2$  itself, not divided by the number of degrees of freedom, has improved notably. This fact allows us to conclude about the data fit improvement, at least for some ratios. As one can see from Figs. 1 and 2, the temperature, baryo-chemical potential, and chemical potential of the isospin third projection obtained for the  $\gamma_s$  fit demonstrate almost the same behavior as for the case of the chemical FO model with  $\gamma_s = 1$ .

The comparison between the parametrized behavior of the  $T(\sqrt{s_{NN}})$  and  $\mu_B(\sqrt{s_{NN}})$  dependences suggested in [33] and our results is shown in Fig. 1. The functions  $T(\sqrt{s_{NN}})$  and  $\mu_B(\sqrt{s_{NN}})$  suggested in [33] are given by

$$T[\text{MeV}] = \frac{T_{\text{lim}}}{1 + \exp[2.6 - \ln(\sqrt{s_{NN}})/0.45]}, \quad (6)$$

$$\mu_B[\text{MeV}] = \frac{1303}{1 + 0.286\sqrt{s_{NN}}}, \quad (7)$$

where the collision energy  $\sqrt{s_{NN}}$  is measured in GeV. Here, the value of “limiting” temperature  $T_{\text{lim}}$  is 164 MeV [33]. Note that the parametrized chemical potential behavior is in a good correspondence with the results obtained in this work. On the other hand, we found lower values for the chemical FO temperature comparing to [33] in our model, and the results coincide only for the highest RHIC energies. Apparently, such a difference in the chemical FO temperatures seen at low collision energies is mainly due to different values of the hard-core radii used here and in [33].

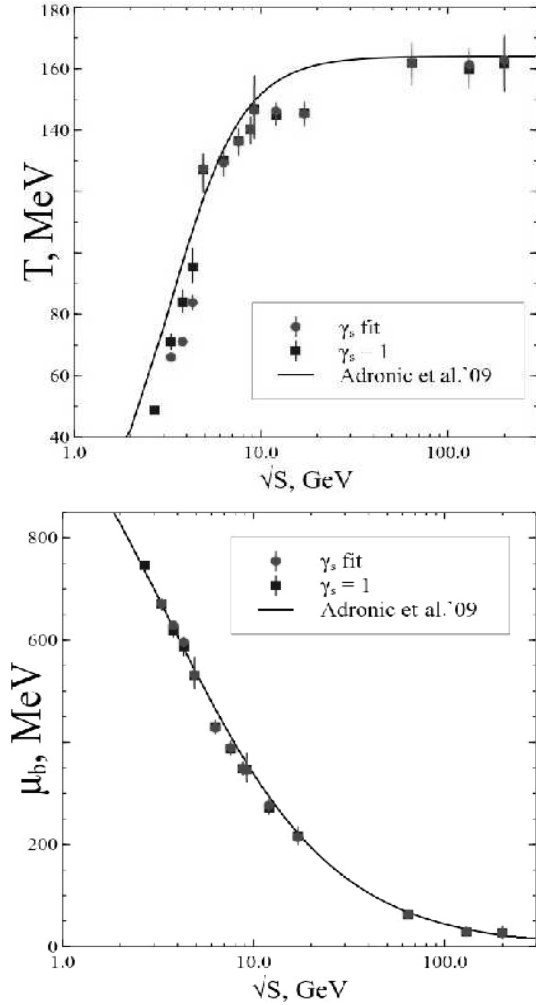


**Fig. 1.** Comparison of the behaviors of parameters for the  $\gamma_s$  fit, chemical FO model with  $\gamma_s = 1$ , and Adronic *et al.* results from [33]. Upper panel: the chemical FO temperature  $T$ . Lower panel: the chemical FO baryo-chemical potential  $\mu_B$

The most remarkable behavior is demonstrated by the  $\gamma_s(\sqrt{s_{NN}})$  function (see the lower panel of Fig. 2). In contrast to the earlier results [3], we found not a strangeness suppression, but a sizable enhancement ( $\gamma_s > 1$ ) at the energies below  $\sqrt{s_{NN}} = 8.8$  GeV, while our results  $\gamma_s \simeq 1$  are consistent at higher energies with the findings of Ref. [6]. We have to stress that our results on the  $\gamma_s$  fit have very high quality. This is clearly seen in Figs. 3, 4, and 5. At the same time, the results of Ref. [3] have typical values of  $\chi^2/\text{dof}$  between 2 and 5 at each energy point, while our value  $\chi^2/\text{dof} = 63.4/55 = 1.15$  is given for all 111 indepen-

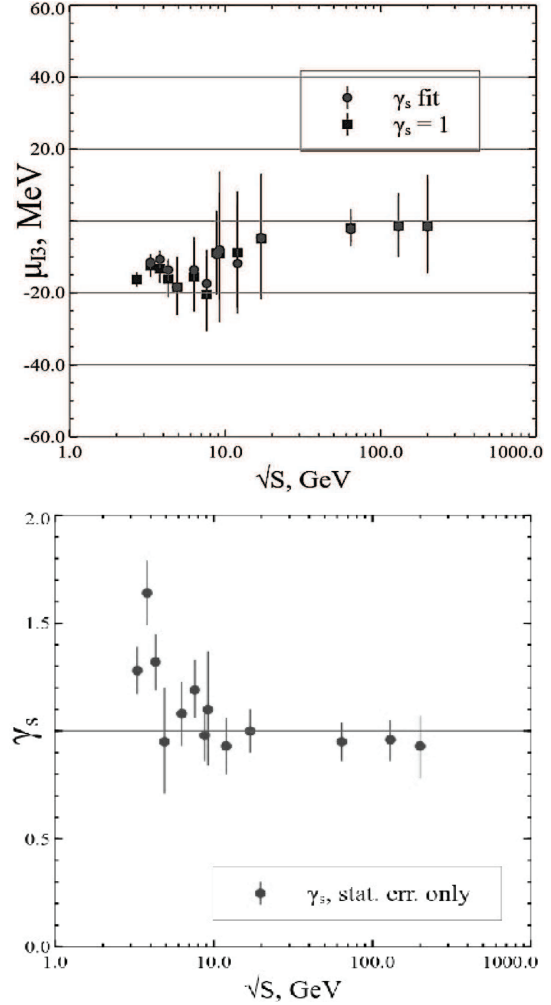


**Fig. 2.** Same as in Fig. (1), but for the chemical potential of the third projection of isospin  $\mu_{I3}$  (upper panel) and the strangeness enhancement factor  $\gamma_s$  (lower panel)

dent ratios measured at 14 energies. Therefore, we conclude that the results on the strangeness suppression in heavy ion collisions reported in [3] are based on a low quality fit, and, hence, they cannot be regarded as the statistically confident ones.

We now study which ratios are improved at various energies. For AGS energies  $\sqrt{s_{NN}} = 2.7, 3.3, 3.8,$  and  $4.3$  GeV, the description quality is quite good even within the ideal gas model [2], since the number of model parameters is equal or almost equal to the available number of ratios, and only kaons and  $\Lambda$  contain strange quarks. Our detailed analysis demonstrates the fit instability for the low energies due to

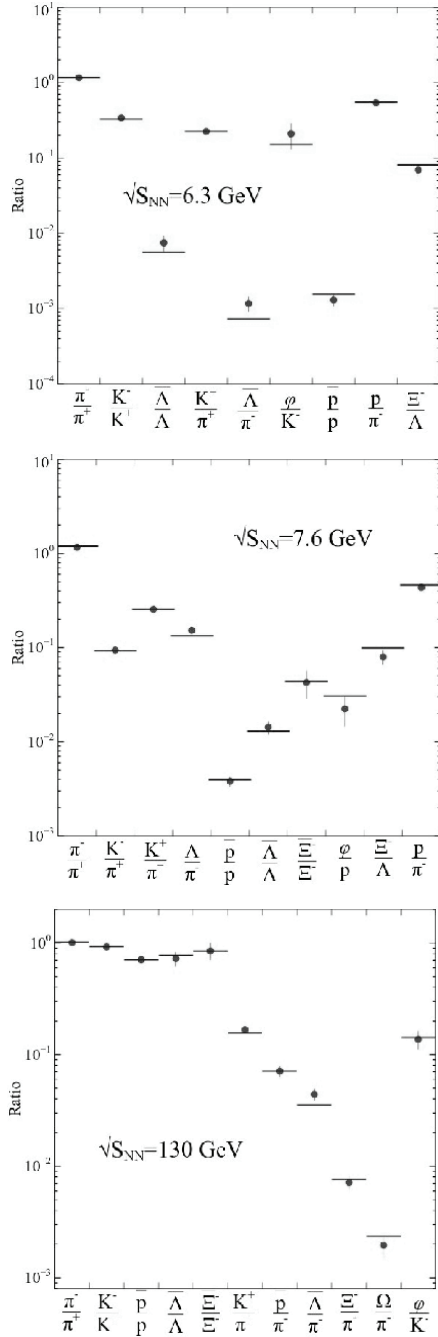


**Fig. 3.** Examples of the description of particle yield ratios obtained for the  $\gamma_s$  fit. The dots denote the experimental values, while the lines show the fitting results. The symbols on the OX axis demonstrate the particle ratios. Upper panel:  $\sqrt{s_{NN}} = 6.3$  GeV,  $T = 129$  MeV,  $\mu_b = 427$  MeV. Middle panel:  $\sqrt{s_{NN}} = 7.6$  GeV,  $T = 136$  MeV,  $\mu_b = 389$  MeV. Lower panel:  $\sqrt{s_{NN}} = 130$  GeV,  $T = 161$  MeV,  $\mu_b = 29$  MeV

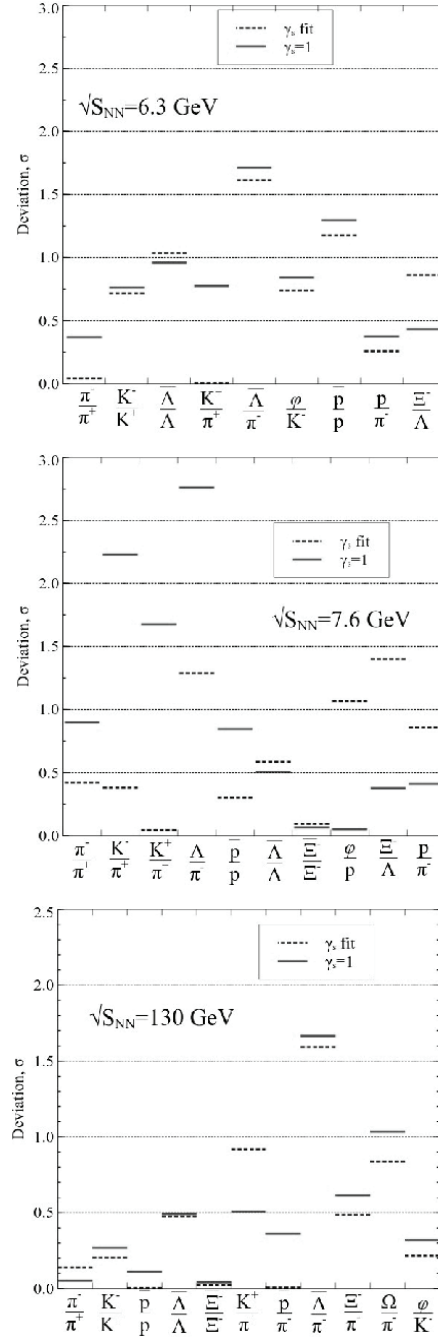


**Fig. 4.** Relative deviation of the theoretical description of ratios from the experimental value in units of experimental error  $\sigma$ . The symbols on the OX axis demonstrate the particle ratios. The OY axis shows  $\frac{|r^{\text{theor}} - r^{\text{exp}}|}{\sigma^{\text{exp}}}$ , i.e. the moduli of relative deviations for  $\sqrt{s_{NN}} = 6.3, 7.6,$  and  $130$  GeV. Solid lines correspond to the model of chemical FO with  $\gamma_s = 1$ , while the dashed lines correspond to the model with the  $\gamma_s$  fit

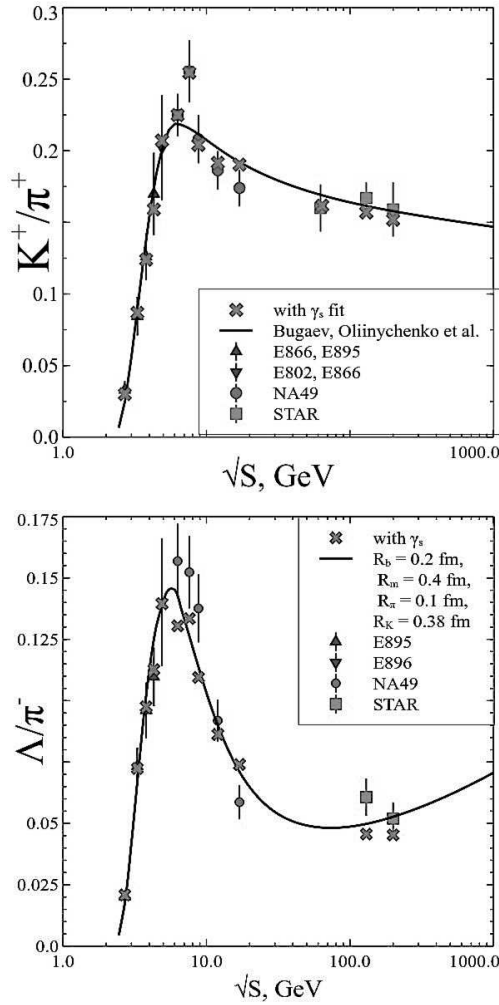


**Fig. 5.** Description of the  $K^+/\pi^+$  (upper plot) and  $\Lambda/\pi^-$  ratios (lower plot). Solid lines show the results of [4] for the HRGM with  $\gamma_s = 1$ . Crosses stand for the case of the  $\gamma_s$  fit

the existence of two local minima with very close  $\chi^2$  values. Thus, for  $\sqrt{s_{NN}} = 3.8$  GeV, we obtained  $\gamma_s \simeq 1.6$  for the deepest minimum, while, for another minimum next to the deepest one,  $\gamma_s \simeq 0.8$ . During the fit procedure, only the deepest minima were considered. The existence of two local minima with close values of  $\chi^2$  at  $\sqrt{s_{NN}} = 2.7\text{--}4.3$  GeV allows us to conclude [10] that the  $\gamma_s$  concept has to be refined further in order to resolve this problem.

For the collision energy  $\sqrt{s_{NN}} = 4.9$  GeV, there are no sizeable improvements compared to the  $\gamma_s = 1$  approach [4]. The most significant data fit improvements are shown in Figs. 3 and 4. At the energies

$\sqrt{s_{NN}} = 6.3\text{--}12$  GeV, the  $K^+/\pi^+$  ratio is notably improved, while the description of other ratios was improved only slightly or even got worse. The typical examples of such a behavior are shown in the upper and middle panels of Fig. 4. At the same time, for the collision energy  $\sqrt{s_{NN}} = 130$  GeV, we find the opposite data description behavior. The lower panel of Fig. 4 clearly demonstrates a fit quality improvement for all ten ratios except for the  $K^+/\pi^+$  ratio.

The obtained overall value  $\chi^2/\text{dof} \simeq 1.15$  for the  $\gamma_s$  fit is only slightly better compared to the result  $\chi^2/\text{dof} \simeq 1.16$  found in [4], although the value of  $\chi^2$  itself, not divided by the number of degrees of freedom, is essentially improved from the value  $\chi^2 \simeq 80.5$  reported in [4] to the value  $\chi^2 \simeq 63.4$  found here.

Nevertheless, the  $\gamma_s$  fit does not essentially improve either the ratios with the multistrange baryons or the  $\Lambda/\pi^-$  ratio (see the lower panel on Fig. 5) which is a consequence of the  $\bar{\Lambda}$  anomaly reported in [34, 35]. Hence, we believe that a further improvement of the data description is possible. However, an important result of the  $\gamma_s$  fitting approach is a precise Strangeness Horn description with  $\chi^2/\text{dof} = 3.3/14$ , i.e. essentially better than it was done in [4] with  $\chi^2/\text{dof} = 7.5/14$ . Even the highest point of the Strangeness Horn is perfectly described now, which makes our theoretical Strangeness Horn as sharp as an experimental one (see the upper panel of Fig. 5). Therefore, we consider the high quality of the  $K^+/\pi^+$  ratio description as an additional important criterion in favor of the  $\gamma_s$  fit.

#### 4. Conclusions

We present an advanced description of the experimental hadron multiplicity ratios measured at AGS, SPS, and RHIC energies. The inclusion of the  $\gamma_s$  factor into the recently developed version of the HRGM with the multicomponent hard-core repulsion has essentially improved the Strangeness Horn description to  $\chi^2/\text{dof} = 3.3/14$ , i.e. better than it was done recently in [4] with  $\chi^2/\text{dof} = 7.5/14$  and much better than it was done in [1–3, 6]. For the first time, even the highest point of the Strangeness Horn is perfectly reproduced by our HRGM, which makes our theoretical horn as sharp as an experimental one. In contrast to the earlier results reported in [3], we find that, in heavy ion collisions, there is a sizable enhancement of the strangeness at low collision energies with  $\gamma_s \simeq 1.2\text{--}1.6$ . The achieved high quality fit of

hadronic multiplicities with  $\chi^2/\text{dof} \simeq 63.5/55 \simeq 1.15$  gives us a high confidence in our conclusions. However, the present analysis shows that the  $\gamma_s$  fit does not sizably improve the description of the multi-strange baryons and antibaryons. Therefore, we conclude that the alternative approaches to the chemical FO suggested in [10, 36] should be developed further. We hope that the high quality data expected to be measured at the future heavy ion facilities will help us to understand the reason for the apparent chemical non-equilibrium of the strange charge.

We have performed a thorough analysis of two alternative approaches to treat the chemical freeze-out of strange particles in the hadron resonance gas model with the multicomponent hard-core repulsion [1]. The first approach accounts for their chemical non-equilibrium via the usual  $\gamma_s$  factor, and such a model describes the hadron multiplicities measured in nucleus-nucleus collisions at AGS, SPS, and RHIC energies with  $\chi^2/\text{dof} \simeq 63.5/55 \simeq 1.15$ . In contrast to earlier beliefs, we find that the strangeness rather tends to be enhanced than suppressed at low collision energies, i.e.  $\gamma_s > 1$ , at  $\sqrt{s_{NN}} = 2.7, 3.3, 3.8, 4.9, 6.3,$  and  $9.2$  GeV. The second approach is to treat the strange particle freeze-out separately from the non-strange particle freeze-out. Conservation laws allow us to connect the freeze-outs of strange and non-strange hadrons and end up with the same number of free parameters as for the  $\gamma_s$  approach. We show that this approach works not worse than the  $\gamma_s$  approach with  $\chi^2/\text{dof} \simeq 58.5/55 \simeq 1.06$ , and, for  $\sqrt{s_{NN}} = 6.3, 12,$  and  $17$  GeV, it significantly improves the fit quality. For all considered collision energies, we see that  $\bar{p}/\pi^-, \bar{\Lambda}/\Lambda, \bar{\Xi}^-/\Xi^-,$  and  $\bar{\Omega}/\Omega$  ratios are described better than within the traditional  $\gamma_s$  approach, since the separation of chemical freeze-outs relaxes the strong connection between the non-strange and strange baryons. The novel concept of strange particle freeze-out allows us to describe 111 independent hadron ratios measured at 14 different energies with the highest quality ever achieved. Based on these results, we conjecture that the apparent strangeness enhancement is due to the separate strangeness chemical freeze-out.

*We would like to thank A. Andronic for providing the access to well-structured experimental data. K.A.B., D.R.O., A.I.I., and V.V.S. acknowledge a partial support of the Program "On Perspective Fun-*

*damental Research in High Energy and Nuclear Physics" launched by the Section of Nuclear Physics of the NAS of Ukraine. K.A.B. and I.N.M. acknowledge also a partial support provided by the Helmholtz International Center for FAIR within the framework of the LOEWE program launched by the State of Hesse.*

1. P. Braun-Munzinger, K. Redlich, and J. Stachel, in: *Quark Gluon Plasma*, edited by R.C. Hwa *et al.* (World Scientific, Singapore, 2003), p. 491.
2. A. Andronic, P. Braun-Munzinger and J. Stachel, Nucl. Phys. A **772**, 167 (2006) and references therein.
3. F. Becattini, J. Manninen and M. Gazdzicki, Phys. Rev. C **73**, 044905 (2006).
4. K.A. Bugaev, D.R. Oliinychenko, A.S. Sorin and G.M. Zinovjev, Eur. Phys. J. A **49**, 30–1-8 (2013) and references therein.
5. J. Rafelski, Phys. Lett. B **62**, 333 (1991).
6. P. Braun-Munzinger, D. Magestro, K. Redlich, and J. Stachel, Phys. Lett. B **518**, 41 (2001).
7. G. Zeeb, K.A. Bugaev, P.T. Reuter, and H. Stöcker, Ukr. J. Phys. **53**, 279 (2008).
8. D.R. Oliinychenko, K.A. Bugaev, and A.S. Sorin, Ukr. J. Phys. **58**, 211 (2013).
9. K.A. Bugaev, D.R. Oliinychenko, and A.S. Sorin, Ukr. J. Phys. **58**, 939 (2013).
10. K.A. Bugaev, D.R. Oliinychenko, J. Cleymans, A.I. Ivanytskyi, I.N. Mishustin, E.G. Nikonov, and V.V. Sagun, Europhys. Lett. **104**, 22002 (2013).
11. K.A. Bugaev, A.I. Ivanytskyi, D.R. Oliinychenko, E.G. Nikonov, V.V. Sagun, and G.M. Zinovjev, arXiv:1312.4367 [hep-ph].
12. S. Wheaton, J. Cleymans, and M. Hauer, Comput. Phys. Commun. **180**, 84 (2009).
13. J.L. Klay *et al.*, Phys. Rev. C **68**, 054905 (2003).
14. L. Ahle *et al.*, Phys. Lett. B **476**, 1 (2000).
15. B.B. Back *et al.*, Phys. Rev. Lett. **86**, 1970 (2001).
16. J.L. Klay *et al.*, Phys. Rev. Lett. **88**, 102301 (2002).
17. C. Pinkenburg *et al.*, Nucl. Phys. A **698**, 495c (2002).
18. P. Chung *et al.*, Phys. Rev. Lett. **91**, 202301 (2003).
19. S.V. Afanasiev *et al.*, Phys. Rev. C **66**, 054902 (2002).
20. S.V. Afanasiev *et al.*, Phys. Rev. C **69**, 024902 (2004).
21. T. Anticic *et al.*, Phys. Rev. Lett. **93**, 022302 (2004).
22. S.V. Afanasiev *et al.*, Phys. Lett. B **538**, 275 (2002).
23. C. Alt *et al.*, Phys. Rev. Lett. **94**, 192301 (2005).
24. S.V. Afanasiev *et al.*, Phys. Lett. B **491**, 59 (2000).
25. B. Abelev *et al.*, Phys. Rev. C **81**, 024911 (2010).
26. B. Abelev *et al.*, Phys. Rev. C **79**, 034909 (2009).
27. J. Adams *et al.*, Phys. Rev. Lett. **92**, 182301 (2004).
28. J. Adams *et al.*, Phys. Lett. B **567**, 167 (2003).
29. C. Adler *et al.*, Phys. Rev. C **65**, 041901(R) (2002).
30. J. Adams *et al.*, Phys. Rev. Lett. **92**, 112301 (2004).
31. J. Adams *et al.*, Phys. Lett. B **612**, 181 (2005).
32. A. Billmeier *et al.*, J. Phys. G **30**, S363 (2004).
33. A. Andronic, P. Braun-Munzinger, and J. Stachel, arXiv: 0911.4931 [nucl-th].
34. B.B. Back *et al.*, Phys. Rev. Lett. **87**, 242301 (2001).

35. J. Stachel, A. Andronic, P. Braun-Munzinger, and K. Redlich, arXiv: 1311.4662 [nucl-th].  
36. K.A. Bugaev, D.R. Oliinychenko, V.V. Sagun, A.I. Ivanytskyi, J. Cleymans, E.G. Nikonov, and G.M. Zinovjev, arXiv: 1312.5149 [hep-ph].

Received 02.03.14

*В.В. Сагун, Д.Р. Олійниченко,  
К.О. Бугаєв, Ж. Клейманс, О.І. Іваницький,  
І.М. Мішустін, Є.Г. Ніконов*

#### ПІДСИЛЕННЯ ДИВНОСТІ В АДРОННОМУ ХІМІЧНОМУ ФРІЗАУТІ

#### Резюме

На основі реалістичної версії моделі адронного резонансного газу досліджено хімічний фрізаут адронів, утворених у зіткненнях ядер при високих енергіях. Хімічна нерівнова-

га дивних частинок враховується за допомогою введення  $\gamma_s$  фактора, який дозволяє здійснити високоякісний фіт відношень адронних множинностей, виміряних в інтервалі енергій від найнижчих енергій АGS до найвищих енергій RHIC, із  $\chi^2/\text{dof} \simeq 63,5/55 \simeq 1,15$ . На відміну від попередніх результатів, при низьких енергіях ми спостерігаємо посилення дивності, а не її пригнічення. Крім того, за допомогою проведеного фітування параметра  $\gamma_s$  вдалося досягнути найякіснішого опису Піка Дивності із  $\chi^2/\text{dof} = 3,3/14$ . Вперше вдалося відтворити найвищу точку Піка Дивності, що робить теоретичний Пік настільки ж гострим, як і експериментальний. Проте, проведене фітування  $\gamma_s$  не призвело до суттєвого покращення опису мультидивних баріонів та антибаріонів. Тому, видиме відхилення мультидивних баріонів та антибаріонів від хімічної рівноваги вимагає додаткового пояснення.